Phase equilibrium measurements and thermodynamic modeling of {CO$_2$ + diethyl succinate + cosolvent} systems

Amabille Petza Kloc[1], Eleni Grilla[2], Claudia A. Capeletto[1], Maria Papadaki[3], Marcos L. Corazza*[,1]

[1] *Department of Chemical Engineering, Federal University of Paraná, 81531-980 Curitiba-PR, Brazil.*

[2]*Department of Chemical Engineering, University of Patras, GR-26504 Patras, Greece*

[3]*Department of Environmental Engineering, University of Patras, Seferi 2, GR-30100 Agrinio, Greece*

Corresponding author:

Dr. Marcos Lúcio Corazza

Department of Chemical Engineering

Federal University of Paraná, Polytechnique Center

PO BOX. 19011

Curitiba 81531-980, State of Paraná, Brazil.

Email: corazza@ufpr.br

Telephone: + 55-41-33613587

1   Abstract

2   This work reports experimental phase equilibrium data for the binary systems $\{CO_2(1) +$

3   diethyl succinate(2)$\}$ and $\{CO_2(1) +$ ethyl acetate(2)$\}$, and for the ternary systems $\{CO_2(1)$

4    $+$ diethyl succinate(2) $+$ ethanol(3)$\}$ and $\{CO_2(1) +$ diethyl succinate(2) $+$ ethyl acetate(3)$\}$.

5   The experiments for the binary system $\{CO_2(1) +$ diethyl succinate(2)$\}$ were carried out at

6   temperatures ranging from 308 K to 358 K, and temperatures ranging from 303 K to 343 K

7   for $\{CO_2(1) +$ ethyl acetate(2)$\}$ as well as for all ternary systems. Only vapor-liquid

8   equilibria were observed for all systems. The experimental measurements were carried out

9   in a high-pressure variable-volume view cell containing a movable piston, which allows

10   pressure control inside the cell. Binary and ternary systems were modeled with the Peng-

11   Robinson cubic equation of state with the van der Waals quadratic mixing rule (vdW2).

12   The presence of a cosolvent (ethanol and ethyl acetate) decreased the saturation pressures

13   of either bubble or dew points compared to the binary system CO_2 + diethyl succinate,

14   increasing the solubility of diethyl succinate in CO_2.

15

16   **Keywords:** Diethyl succinate, cubic equation of state, supercritical CO_2, high-pressure,

17   VLE measurement.

18

19

1. Introduction

Diethyl succinate (DES) is a diester that occurs naturally in plants. It can be used as a flavoring agent, in fragrances, synthesis of polyesters, plasticizers, food additives, chemical intermediates [1–4], and as a solvent to recover carboxylic acids [5]. A potential method of recovery of DES from plants is via extraction with supercritical carbon dioxide ($scCO_2$). On the other hand, esters such as DES can be synthesized from the esterification of carboxylic acids either catalyzed by enzymes or chemical catalysts in $scCO_2$ medium [6–9]. Another very promising process involving is the CO_2 capture with DES as solvent [10]. In all these processes mentioned, a cosolvent use can be an interesting technical strategy in order to enhance the DES solubility in CO_2 at high pressure conditions or to promote a synergic effect of mixed solvents. However, phase equilibrium data are imperative for the design of a larger scale process. Phase equilibrium data at high pressures for supercritical fluid systems are scarce and as supercritical fluid applications are increasing, the collection of such data has becoming more important. Supercritical carbon dioxide in particular has been widely studied as a promising alternative solvent for chemical reaction and separation processes because it is nontoxic, inexpensive, easily recycled and has low critical temperature and pressure ($T_c = 304.2$ K, $P_c = 7.38$ MPa, respectively) [11]. Favorable large-scale application solvents should ideally be highly selective, non-viscous, chemically stable and non-corrosive. CO_2 fulfills these requirements. Moreover, as opposed to organic chemical solvents such as methanol, propylene carbonate, and polyethylene glycol dimethyl ether (Selexol) the recovery of which in the desorption stage can be problematic and/or energy intensive, CO_2 can be easily recovered by a change in temperature or pressure in the

1   desorption process [10]. Thus, it forms an effective and low-cost physical absorbent,

2   suitable for large-scale industrial applications.

3   Literature has reported that diethyl succinate (DES) is considered an environmentally

4   adequate solvent because of its low volatility and nearly zero solvent loss, as stated by Li et

5   al. [10]. Feng et al. [3] presented vapor-liquid equilibrium (VLE) data from 308.15 to

6   328.15 K and pressures up to 13 MPa for the system CO_2+DES using a semi-flow type

7   apparatus. Li et al. [10] used a gas-phase recirculation method to determine the VLE data

8   from 288.15 to 318.15 K and pressures up to 2.99 MPa. Gui et al. [12] used the constant-

9   volume method to perform VLE experiments at different temperatures in the range of

10   285.19 to 313.26 K and up to 6 MPa. However, a high discrepancy between the VLE data

11   of CO_2 + DES presented by those authors can be noted; the most likely reason for such

12   differences in the phase equilibrium measured is because they used a technique with phase

13   sampling. To the best of our knowledge none of the VLE binary data of CO_2 + DES

14   reported in the literature were not taken using a synthetic variable-volume view cell

15   (without sampling). Furthermore, no experimental information has been reported on ternary

16   systems involving CO_2 + DES + cosolvents.

17   In this context, the main goal of this work is to report experimental phase equilibrium

18   data for the binary systems {CO_2(1)+DES(2)} and {CO_2(1)+ ethyl acetate(2)} and for the

19   ternary systems {CO_2(1) + DES(2) + ethanol(3)} and {CO_2(1) + DES(2) + ethyl

20   acetate(3)}. The experimental results for the systems investigated were modeled using the

21   Peng-Robinson equation of state (PR-EoS) with the conventional quadratic van der Waals

22   mixing rule (vdW2).

23

24

2. Experimental

2.1 Materials

All chemicals employed in this study, their purity, and supplier are presented in Table 1. All compounds were used without further purification.

Table 1

2.2 Apparatus and experimental procedure

The experimental apparatus and procedure used in this work were presented and described in previous publications [13–17]. Briefly, the experimental data measurements were performed in a high-pressure variable-volume view cell containing a movable piston, which allows the pressure control inside the cell. The apparatus also includes a syringe pump (ISCO, model 260D) for the CO_2 injection into the equilibrium cell and for manipulating pressure into the cell and an electrical heating jacket for the temperature control. A pressure transducer (Smar, model LD 301, with the uncertainty of $\pm$ 0.03 MPa) and a universal indicator (Novus, model N1500) are coupled in the unit for pressure data measurement, and a thermocouple (K-type) to measure and register the temperature inside the cell. The visual observations were achieved through two sapphire windows, one on the side and another on the front. The experimental procedure consisted of flushing the cell with CO_2 (288.15 K and 6.5 MPa) to remove any residual air and after that loading the cell with the respective amount of liquid solute (pure compounds or a mixture of solutes at a

1   fixed composition). After adding the known amount of solute into the cell, the CO_2 was

2   loaded at fixed conditions of temperature and pressure in the syringe pump (288.15 K and

3   10 MPa). Once the equilibrium cell was loaded with a mixture of fixed and known

4   composition, the temperature was fixed at the desired setpoint. Subsequently, the pressure

5   was increased to reach a homogeneous phase. After that, the phase transition pressure (the

6   phase saturation condition) was measured by decreasing the pressure at a constant rate (0.3

7   MPa min^{-1}) until the formation of a new and incipient phase was observed. The procedure

8   of pressurizing to the homogeneous-phase conditions and systematically decreasing the

9   pressure to get the formation of a new phase was repeated three times. The reading values

10 were averaged and standard deviations for the saturation pressure and temperature were

11 calculated. These values are reported along with the average values of pressure and

12 temperature in tables containing the experimental data. However, as these repetitions

13 represent the reading variations (deviations), which are essential to assess the variance

14 related to thermal and mechanical perturbations of the system (since the system was

15 considered to be at equilibrium at all measurements), we further considered type B

16 uncertainties, namely the uncertainties estimated using previous measurements,

17 manufacturer specifications, sensors hysteresis, calibrations, etc. (for more information see

18 Taylor and Kuyatt [18]). Thus, type B uncertainties related to the mole fraction,

19 temperature and pressure measurements are also reported in tables (footnotes) with the

20 experimental data.

21

22 **3. Thermodynamic modeling**

1   The Peng-Robinson equation of state (PR-EoS) [19], with the conventional quadratic

2   van der Waals mixing rule (vdW2) for both attractive (*a*) and repulsive (*b*) terms (equations

3   1 and 2) was used in this work for modeling the VLE data of both binary and ternary

4   systems investigated.

5

6       $$a = \sum_i \sum_j x_i x_j \sqrt{a_i a_j} \left(1 - k_{ij}\right)$$ (1)

7

8       $$b = \sum_i \sum_j x_i x_j \left(\frac{b_i + b_j}{2}\right) \left(1 - l_{ij}\right)$$ (2)

9

10   In equations 1 and 2, a_i and b_i stand for pure component parameters related to the PR-EoS

11   [19]. $P_{cal,i}$ and $P_{exp,i}$ represent for the calculated and experimental values of pressure in the "i"

12   measurement. *NOBS* is the number of experimental observations.

13   The estimation of the binary interaction parameters (k_{ij} and l_{ij} in equations 1 and 2,

14   respectively) was carried out by minimizing the least squares objective function of

15   experimental and calculated pressure values (equation 3) using the Nelder-Mead Simplex

16   method from the Matlab optimization toolbox ("fminsearch" subroutine). The calculation

17   of saturation points followed the procedure proposed by Michelsen [20], with modifications.

18   Properties of pure components used in this work are presented in Table 2.

19

1 $$F = \sum_{i=1}^{NOBS} \left(P_{cal,i} - P_{exp,i} \right)^2 \qquad (3)$$

2

3 **Table 2**

4

5 **4. Results and discussion**

6   In order to verify the experimental apparatus and procedure reliability, experimental

7 phase equilibrium data for the system $\{CO_2(1) + \text{ethyl acetate}(2)\}$ were obtained (Table 3)

8 and compared to data available in the literature, as presented in Figure 1. Table 3 presents

9 the reading average temperature (T) and average pressure (P) ± its standard deviations, at a

10 fixed molar composition (x) calculated using the solute mass weighted (± 0.0001 g

11 uncertainty, RADWAG AS220/C/2) and the CO_2 amount injected using the syringe pump

12 measured by the volume variation (16.63 nL uncertainty, ISCO 260D) at a fixed

13 temperature (± 0.05 °C uncertainty, thermostatic circulation bath, VIVO RT4) and pressure

14 (± 0.005 MPa uncertainty, ISCO 260D) obtained in this work. However, the maximum

15 experimental standard uncertainties were estimated considering a type B uncertainty of ±

16 0.20 MPa, ± 0.5 K and 0.005 related to measurements of pressure, temperature and mole

17 composition, respectively (Table 3). Therefore, it can be observed that the present data for

18 the system $\{CO_2(1) + \text{ethyl acetate}(2)\}$ are in agreement with the data reported by Borges et

19 al. [21], Byun et al. [22], and Aida et al.[23], at all temperatures compared. For other

20 references significant differences are noted. It is worth mentioning that the data agreeing

21 were obtained using a synthetic visual method ([21–23]) and the other ones [24–26] were

1   obtained using an analytic method which involved sampling. Data presented by Sima at al.

2   [26], which were also measured using an analytical method seems to be closer to those

3   presented in the present work, mainly at 323 K. However, at higher temperatures deviations

4   up to 1 MPa can also be observed. Further comparing the data evaluated, Tian et al. [27]

5   employed a static synthetic measurement method; the data presented by them agree with

6   those of other authors at 333 K (including the data measured in the present work). However,

7   at 353 K, for the compositions around 0.6 mole fraction of CO_2 the data presented by Tian

8   et al. (blue diamonds) disagree with the data obtained by Byun et al. [22] and those

9   obtained in our work. In addition, the data presented by Tian at al. are crossing when

10   comparing the two temperatures of at 353 K and 333 K, which is not expected for data of a

11   saturated liquid phase. As it can be seen in Figure 1, a substantial discrepancy can be noted

12   between experimental data of phase saturation obtained using a static synthetic and those

13   obtained using analytical methods (with phase sampling). Thus, comparison of data of so

14   different origin must be conducted with special care. A sampling procedure at high pressure

15   and a highly compressible system can cause severe perturbations in the equilibrium of the

16   system. On the other hand, synthetic methods avoid any sampling perturbation.

17   Consequently, it is stated that the synthetic methods without sampling can be more suitable

18   for phase saturation measurements at high pressure and, in general, they can provide more

19   reliable data. In addition, the thermodynamic model used (PR without adjustable parameter,

20    $k_{12} = l_{12} = 0$, Figure 1) is also in excellent agreement with the data measured in this work

21   since the predicted values agree with the experimental data obtained by the synthetic

22   method employed here.

23

1   **Table 3**

2

3   **Figure 1**

4

5   After testing and demonstrating the quality of the data obtained in our experimental

6   apparatus for the aforementioned binary system, phase-equilibrium measurements were

7   conducted for the system $\{CO_2(1) + DES(2)\}$ for temperatures ranged from 308 to 358 K,

8   as presented in Table 4. Tables 5 and 6 present the phase transitions measurements for the

9   ternary systems $\{CO_2(1) + DES(2) + ethanol(3)\}$ and $\{CO_2(1) + DES(2) + ethyl\ acetate(3)\}$,

10   respectively, at different fixed DES to ethanol (or ethyl acetate) molar ratios. These tables

11   express the experimental data in terms of molar compositions of CO_2 (x_1) and solute

12   mixtures at a fixed DES to ethanol (or ethyl acetate) molar ratio, named as $\bar{x}_2$, and its

13   pressure transition measurements (p), at a fixed temperature. As mentioned before, the

14   standard deviation of pressure measurement replicates (σ), and the type of phase

15   equilibrium transition observed, meaning bubble point (BP) or dew point (DP), are also

16   presented.

17

18   **Table 4**

19

20   **Table 5**

21

22   **Table 6**

1

2   In this work, thermodynamic modeling using the PR model was performed by fitting a

3   unique set of binary interaction parameters for all isotherms (global fitting). For each binary

4   system {CO_2(1) + ethyl acetate(2), CO_2(1) + DES(2)}, the attraction energy parameter (k_{ij})

5   and repulsive energy parameter (l_{ij}) are presented in Table 7, as well as the root mean

6   square deviation (*rmsd*) calculated using equation (4).

7

8    $$rmsd = \sqrt{\sum_{i=1}^{NOBS} \left(P_{cal,i} - P_{\exp,i} \right)^2}$$ (4)

9

10

11   **Table 7**

12

13   Figure 2 depicts the pressure-composition diagram for the system {CO_2(1) +

14   DES(2)} at different temperature, where the data obtained in this work are compared with

15   data presented in the literature, as well as the calculated values using the PR model with

16   binary interaction parameters (k_{12} and l_{12}) set to zero and adjusted values (Table 7). Is noted

17   that for this system a difference among the data measured in this work and those presented

18   in the literature, mainly at CO_2 mole fraction above ~ 0.5 (data presented by [3]). The phase

19   equilibrium data presented by Feng et al. [3] were obtained applying a synthetic analytical

20   method with sampling both liquid and vapor phase and it is evident that such method may

21   produce nonreliable data in particular in the range which is closer to the critical point of the

22   mixture.

1   From Figure 2 and the *rmsd* values presented in Table 7, it is possible to see that the

2   PR model with quadratic mixing rule is capable to represent the phase behavior of the

3   system $\{CO_2(1) + DES(2)\}$ for the temperature range investigated in this study. A small

4   correction in the attractive and repulsive energy parameters was enough to reliably capture

5   the molecular interaction between CO_2 and ethyl succinate (DES) ester; a similar

6   performance of the thermodynamic model was observed for the system CO_2 +ethyl acetate.

7

8   **Figure 2**

9

10   *Ternary Systems*

11   Ternary systems were modeled using the aforementioned binary interaction

12   parameters of the systems $CO_2(1)$ + DES(2), $CO_2(1)$ + ethyl acetate(2) and $CO_2(1)$ +

13   ethanol(2); the interaction parameters for the latter, i.e. for CO_2 – ethanol were taken from

14   the literature [29]. The results for the ternary systems $\{CO_2(1) + DES(2) + ethanol(3)\}$ and

15   $\{CO_2(1) + DES(2) + ethyl\ acetate(3)\}$ are presented in Figure 3 and 4, respectively,

16   considering pressure-temperature diagrams at different overall compositions. In these

17   figures, the experimental saturation points are compared with those predicted using the

18   thermodynamic model based on the binary interaction parameters of solute – solute (DES –

19   ethanol and DES – ethyl acetate) set to zero. This approach leads to good predictions of the

20   phase saturation (saturation pressure – bubble points) for these two ternary systems.

21   Consequently, the PR equation of state with the vdW2 mixing rule is capable of

22   representing the thermodynamic interactions of systems $CO_2(1)$ + DES(2) + ethanol(3)$\}$

23   and $\{CO_2(1) + DES(2) + ethyl\ acetate(3)\}$ considering only the interaction between CO_2 -

1   DES, and CO_2 - ethanol and CO_2 - ethyl acetate. As it can be seen, there was no need for

2   correction for the attraction and repulsion energy parameters between DES – ethanol and

3   DES – ethyl acetate at high pressures. Root means deviations (*rmsd*) around 0.4 MPa for

4   both ternary systems (Table 8, $k_{23} = l_{23} = 0$) was observed. However, aiming to represent

5   better the phase behavior of these systems the solute-solute interaction parameters were

6   fitted (using the ternary data) and the results are also presented in Table 8, where it can be

7   seen that the *rmsd* values decreased to 0.24 and 0.17 for the ternary systems containing

8   ethanol and ethyl acetate, respectively. The reduction in the *rmsd* values demanded high

9   values for the interaction parameters of DES – ethanol and DES ethyl acetate, which

10   indicates that intermolecular forces acting in the system are not properly computed by van

11   der Waals forces (hard spheres attraction and repulsion energy), for example, hydrogen

12   bonds or dipole-dipole interactions. Figure 5 presents the dispersion error between

13   experimental (P_{exp}) and calculated values (P_{cal}) considering $k_{23} = l_{23} = 0$, as well as using

14   the adjusted binary interaction parameters. As can be seen in Figure 5, errors are limited to

15   a range around the experimental error assumed (type B). Even when fitting the k_{23} and l_{23},

16   the dispersion is decreased to around zero but still the remaining lack of fit indicates that

17   the model is "missing" some phenomena. Thus, the thermodynamic model with molecular

18   interactions computing intra and intermolecular interactions should be used in order to

19   improve the saturation point prediction for the systems involved in this work. Nonetheless,

20   it is worth emphasizes that a simple (from computation viewpoint) approach using a cubic

21   equation of state with quadratic mixing rule for both *a* and *b* parameters can produce

22   satisfactory results, with maximum deviations around 0.4 MPa.

23

Figure 3

In general, the PR model with two temperature-independent binary interaction parameters resulted in good predictions for the systems $\{CO_2(1) + \text{ethyl acetate}(2)\}$ and $\{CO_2(1) + DES(2)\}$ where CO_2 − ester molecular interactions are present. Further studies concerning the thermodynamic modeling of systems involving CO_2 / esters / carboxylic acids using equations of state based on Statistical Association Fluid Theory (SAFT) are being conducted in our research group for an improved understanding of the molecular interactions and the thermodynamics of these systems.

Figure 4

Table 8

Figure 5

5. Conclusions

This work reported phase equilibrium data for CO_2 + ethyl acetate and CO_2 + diethyl succinate (CO_2 + DES) binary systems at temperatures ranging from 308 K to 358 K, and CO_2 + DES + ethanol and CO_2 + DES + ethyl acetate ternary systems at temperatures

1 ranging from 303 K to 343 K. Vapor-liquid equilibrium data (bubble and dew points) were

2 observed for all binary and ternary systems investigated over the temperature and

3 composition ranges evaluated. All systems were modeled with the Peng-Robinson equation

4 of state with the van der Walls quadratic mixing rule (vdW2), where small corrections in

5 the terms of the attraction (k_{ij}) and repulsion (l_{ij}) parameters leads to excellent predictions

6 of the VLE for the binary systems CO_2 + ethyl acetate and CO_2 + DES, with low values of

7 *rmsd* with a unique set of binary interaction parameters (k_{ij} and l_{ij}), both temperature-

8 independent. From an engineering point of view, the thermodynamic approach used in this

9 work was also capable of predicting the saturation lines (bubble points) of CO_2 + DES +

10 ethanol and CO_2 + DES + ethyl acetate ternary systems using information from binary

11 systems, resulting in good agreement between experiment and theory. Results obtained in

12 this work are very useful for those who are interested in processes involving high-pressure

13 techniques with CO_2 as the solvent and with organic solvents (ethanol, ethyl acetate and

14 DES) related to "green" process concepts.

15

16

17 **Acknowledgments**

1

2

References

[1]   C. Da Porto, D. Decorti, Supercritical CO2 extraction of grappa volatile compounds, Int. J. Food Sci. Technol. (2009). doi:10.1111/j.1365-2621.2009.01999.x.

[2]   J.A.P. Coelho, A.P. Pereira, R.L. Mendes, A.M.F. Palavra, Supercritical carbon dioxide extraction of Foeniculum vulgare volatile oil, Flavour Fragr. J. (2003). doi:10.1002/ffj.1223.

[3]   L.C. Feng, K.W. Cheng, M. Tang, Y.P. Chen, Vapor-liquid equilibria of carbon dioxide with ethyl benzoate, diethyl succinate and isoamyl acetate binary mixtures at elevated pressures, J. Supercrit. Fluids. 21 (2001) 111–121. doi:10.1016/S0896-8446(01)00091-2.

[4]   H. Chen, L. Zhang, Y. Huang, J. Lu, Z. Zhao, X. Wang, Isobaric vapor–liquid equilibrium of three binary systems containing dimethyl succinate, dimethyl glutarate and dimethyl adipate at 2, 5.2 and 8.3 kPa, J. Chem. Thermodyn. 133 (2019) 100–110. doi:10.1016/j.jct.2019.02.006.

[5]   J.A. Belgodere, E.D. Revellame, R. Hernandez, W. Holmes, L. Collazos, R. Bajpai, M.E. Zappi, Liquid-liquid equilibria for (volatile fatty acids + water + alcohol ethoxylates): Experimental measurement of pseudo-ternary systems, J. Chem. Thermodyn. 128 (2019) 207–214. doi:10.1016/j.jct.2018.08.027.

[6]   E.J. Beckman, Supercritical and near-critical CO2 in green chemical synthesis and processing, J. Supercrit. Fluids. (2004). doi:10.1016/S0896-8446(03)00029-9.

[7]   M. Habulin, S. Šabeder, M.A. Sampedro, Ž. Knez, Enzymatic synthesis of citronellol laurate in organic media and in supercritical carbon dioxide, Biochem. Eng. J. (2008). doi:10.1016/j.bej.2008.05.012.

[8]   F. Gasc, S. Thiebaud-Roux, Z. Mouloungui, Methods for synthesizing diethyl carbonate from ethanol and supercritical carbon dioxide by one-pot or two-step reactions in the presence of potassium carbonate, J. Supercrit. Fluids. (2009). doi:10.1016/j.supflu.2009.03.008.

[9]   E. Leino, P. Mäki-Arvela, V. Eta, N. Kumar, F. Demoisson, A. Samikannu, A.R. Leino, A. Shchukarev, D.Y. Murzin, J.P. Mikkola, The influence of various synthesis methods on the catalytic

activity of cerium oxide in one-pot synthesis of diethyl carbonate starting from CO 2, ethanol and butylene oxide, Catal. Today. (2013). doi:10.1016/j.cattod.2013.02.011.

[10] H. Li, Z. Tang, Z. He, J. Cui, D. Guo, Z. Zhao, X. zhong Mao, Performance evaluation of CO 2 capture with diethyl succinate, Appl. Energy. 200 (2017) 119–131. doi:10.1016/j.apenergy.2017.05.036.

[11] R.L. Rowley, W. V. Wilding, J.L. Oscarson, Y. Yang, N.A. Zundel, T.E. Daubert, R.P. Danner, DIPPR data compilation of pure chemical properties, Des. Inst. Phys. Prop. (2003). doi:10.4049/jimmunol.1301009.

[12] X. Gui, W. Wang, C. Wang, L. Zhang, Z. Yun, Z. Tang, Vapor-liquid phase equilibrium data of CO2 in some physical solvents from 285.19 K to 313.26 K, J. Chem. Eng. Data. 59 (2014) 844–849. doi:10.1021/je400985u.

[13] O.A.S. Araújo, F.R. Silva, L.P. Ramos, M.K. Lenzi, P.M. Ndiaye, M.L. Corazza, Phase behaviour measurements for the system (carbon dioxide + biodiesel + ethanol) at high pressures, J. Chem. Thermodyn. 47 (2012) 412–419. doi:10.1016/J.JCT.2011.11.029.

[14] L.F. Pinto, D.I.S. da Silva, F.R. da Silva, L.P. Ramos, P.M. Ndiaye, M.L. Corazza, Phase equilibrium data and thermodynamic modeling of the system (CO2 + biodiesel plus methanol) at high pressures, J. Chem. Thermodyn. 44 (2012) 57–65.

[15] M. V Brandalize, P.S. Gaschi, M.R. Mafra, L.P. Ramos, M.L. Corazza, High-pressure phase equilibrium measurements and thermodynamic modeling for the systems involving CO2, ethyl esters (oleate, stearate, palmitate) and acetone, Chem. Eng. Res. Des. 92 (2014) 2814–2825.

[16] B.A. Veiga, J.T.F. dos Santos, L.F. de Lima Luz Junior, M.L. Corazza, Phase equilibrium measurements and thermodynamic modelling for the systems involving valeric acid, ethanol, ethyl valerate and water plus CO 2, J. Chem. Thermodyn. 112 (2017) 240–248. doi:10.1016/j.jct.2017.05.011.

[17] W.R. Giacomin Junior, C.A. Capeletto, F.A.P. Voll, M.L. Corazza, Phase Equilibrium Measurements and Thermodynamic Modeling of the Systems (CO 2 + Ethyl Levulinate) and (CO 2 + Levulinic Acid), J. Chem. Eng. Data. 64 (2019) 2011–2017. doi:10.1021/acs.jced.8b01023.

[18] B. Taylor, C. Kuyatt, Guidelines for evaluating and expressing the uncertainty of NIST measurement

1   results, (1994).

2   [19]   D.-Y. Peng, D.B. Robinson, A New Two-Constant Equation of State, Ind. Eng. Chem. Fundam. 15

3   (1976) 59–64. doi:10.1021/i160057a011.

4   [20]   M.L. Michelsen, Saturation point calculations, Fluid Phase Equilib. 23 (1985) 181–192.

5   [21]   G.R. Borges, A. Junges, E. Franceschi, F.C. Corazza, M.L. Corazza, J.V. Oliveira, C. Dariva, High-

6   Pressure Vapor−Liquid Equilibrium Data for Systems Involving Carbon Dioxide + Organic Solvent +

7   β-Carotene, J. Chem. Eng. Data. 52 (2007) 1437–1441. doi:10.1021/je700125v.

8   [22]   H.S. Byun, M.Y. Choi, J.S. Lim, High-pressure phase behavior and modeling of binary mixtures for

9   alkyl acetate in supercritical carbon dioxide, J. Supercrit. Fluids. 37 (2006) 323–332.

10   doi:10.1016/j.supflu.2005.10.007.

11   [23]   T. Aida, T. Aizawa, M. Kanakubo, H. Nanjo, Analysis of volume expansion mechanism of CO2-

12   acetate systems at 40 °c, J. Supercrit. Fluids. 55 (2010) 56–61. doi:10.1016/j.supflu.2010.06.002.

13   [24]   Z. Wagner, J. Pavlíček, Vapour-liquid equilibrium in the carbon dioxide-ethyl acetate system at high

14   pressure, Fluid Phase Equilib. 97 (1994) 119–126. doi:10.1016/0378-3812(94)85010-0.

15   [25]   M.V. Da Silva, D. Barbosa, P.O. Ferreira, J. Mendonça, High pressure phase equilibrium data for the

16   systems carbon dioxide/ethyl acetate and carbon dioxide/isoamyl acetate at 295.2, 303.2 and 313.2 K,

17   Fluid Phase Equilib. 175 (2000) 19–33. doi:10.1016/S0378-3812(00)00439-8.

18   [26]   S. Sima, V. Feroiu, D. Geană, New high pressure vapor–liquid equilibrium data and density

19   predictions for carbon dioxide+ethyl acetate system, Fluid Phase Equilib. 325 (2012) 45–52.

20   doi:10.1016/j.fluid.2012.03.028.

21   [27]   Y.L. Tian, H.G. Zhu, Y. Xue, Z.H. Liu, L. Yin, Vapor-liquid equilibria of the carbon dioxide + ethyl

22   propanoate and carbon dioxide + ethyl acetate systems at pressure from 2.96 MPa to 11.79 MPa and

23   temperature from 313 K to 393 K, J. Chem. Eng. Data. 49 (2004) 1554–1559. doi:10.1021/je034224j.

24   [28]   G.R. Borges, A. Junges, E. Franceschi, F.C. Corazza, M.L. Corazza, J.V. Oliveira, C. Dariva, High-

25   pressure vapor-liquid equilibrium data for systems involving carbon dioxide + organic solvent + β-

26   carotene, J. Chem. Eng. Data. (2007). doi:10.1021/je700125v.

27   [29]   O.A.S. Araújo, F.R. Silva, L.P. Ramos, M.K. Lenzi, P.M. Ndiaye, M.L. Corazza, Phase behaviour

28   measurements for the system (carbon dioxide+biodiesel+ethanol) at high pressures, J. Chem.

1   Thermodyn. 47 (2012) 412–419. doi:10.1016/j.jct.2011.11.029.

2

3

1   **Table 1**

2   Chemicals used in this work, their suppliers and mass fraction purity.

Chemical	Supplier	Purity*
Carbon dioxide (CO_2)	White Martins	99.9 wt%
Ethanol (EtOH)	Honeywell	≥ 99.8 wt%
Ethyl Acetate (EA)	Honeywell	≥ 99.95 wt%
Ethyl succinate (DES)	Sigma-Aldrich	≥ 99 wt%

3   *As informed by the suppliers.

4

5

6

7   **Table 2**

8   Characteristic thermodynamic parameters for pure compounds employed in this work.

Compound	T_c/K	p_c/MPa	ω	M_w/(g mol^{-1})	Ref.
CO_2	304.21	7.383	0.22362	44.01	[21]
Ethanol	514.0	6.137	0.64356	46.069	[21]
Ethyl Acetate	523.3	3.88	0.36641	88.106	[21]
Ethyl Succinate	663.0	2.53	0.69951	174.197	[21]

9   T_c, critical temperature; p_c, critical pressure; ω, acentric factor; M_w, molar mass.

10

11

12

13

14

15

16

17

1 **Table 3**

2 Phase equilibrium measurements for the binary system {CO_2(1) + ethyl acetate(2)}.

x_1	p/MPa	σ/MPa	Transition type	x_1	p/MPa	σ/MPa	Transition type
$T = 303.55 \pm 0.30$ K							
0.4065	2.36	0.10	VLE(BP)	0.7018	4.38	0.10	VLE(BP)
0.4841	2.87	0.10	VLE(BP)	0.8221	5.02	0.10	VLE(BP)
0.6092	3.53	0.10	VLE(BP)				
$T = 313.18 \pm 0.31$ K							
0.4065	2.65	0.10	VLE(BP)	0.7018	5.08	0.10	VLE(BP)
0.4841	3.35	0.10	VLE(BP)	0.8221	6.08	0.04	VLE(BP)
0.6092	4.16	0.10	VLE(BP)				
$T = 323.21 \pm 0.12$ K							
0.4065	3.03	0.10	VLE(BP)	0.7018	5.72	0.04	VLE(BP)
0.4841	3.84	0.10	VLE(BP)	0.8221	7.16	0.02	VLE(BP)
0.6092	4.94	0.10	VLE(BP)				
$T = 333.23 \pm 0.25$ K							
0.4065	3.54	0.10	VLE(BP)	0.7018	6.68	0.07	VLE(BP)
0.4841	4.41	0.10	VLE(BP)	0.8221	8.29	0.08	VLE(BP)
0.6092	5.75	0.10	VLE(BP)				
$T = 353.43 \pm 0.28$ K							
0.4065	4.55	0.10	VLE(BP)	0.7018	8.59	0.05	VLE(BP)
0.4841	5.69	0.10	VLE(BP)	0.8221	10.53	0.01	VLE(BP)
0.6092	7.47	0.10	VLE(BP)				

3 Standard uncertainties u are $u(T) = 0.5$ K, $u(p) = 0.20$ MPa, $u(x) = 0.005$. σ/MPa represents the standard
4 deviation of triplicate measurements of phase transitions. VLE(BP) represents bubble point transitions and
5 VLE(DP) dew point transitions.

6

7

8

1 **Table 4**

2 Phase equilibrium measurements for the binary system $\{CO_2(1) + DES(2)\}$.

x_1	p/MPa	σ/MPa	Transition type	x_1	p/MPa	σ/MPa	Transition type
$T = 308.21 \pm 0.18$ K							
0.4246	2.46	0.01	VLE(BP)	0.9008	6.90	0.02	VLE(BP)
0.5484	3.44	0.10	VLE(BP)	0.9483	7.38	0.01	VLE(BP)
0.7024	4.95	0.04	VLE(BP)	0.9925	7.69	0.00	VLE(BP)
0.8052	6.06	0.01	VLE(BP)				
$T = 318.24 \pm 0.24$ K							
0.4246	2.88	0.04	VLE(BP)	0.9008	8.24	0.00	VLE(BP)
0.5484	4.48	0.10	VLE(BP)	0.9483	8.91	0.02	VLE(BP)
0.7024	6.07	0.08	VLE(BP)	0.9925	8.99	0.00	VLE(DP)
0.8052	7.36	0.08	VLE(BP)				
$T = 328.23 \pm 0.37$ K							
0.4246	3.40	0.10	VLE(BP)	0.9008	9.93	0.04	VLE(BP)
0.5484	5.03	0.05	VLE(BP)	0.9483	10.72	0.04	VLE(BP)
0.7024	7.23	0.05	VLE(BP)	0.9925	10.39	0.10	VLE(DP)
0.8052	8.53	0.06	VLE(BP)				
$T = 337.91 \pm 0.18$ K							
0.4246	3.81	0.10	VLE(BP)	0.9008	11.62	0.02	VLE(BP)
0.5484	5.34	0.10	VLE(BP)	0.9483	12.57	0.03	VLE(BP)
0.7024	8.22	0.03	VLE(BP)	0.9925	11.67	0.03	VLE(DP)
0.8052	10.15	0.06	VLE(BP)				
$T = 348.13 \pm 0.14$ K							
0.4246	4.53	0.01	VLE(BP)	0.9008	13.57	0.01	VLE(BP)
0.5484	6.25	0.03	VLE(BP)	0.9483	14.45	0.09	VLE(BP)
0.7024	9.52	0.10	VLE(BP)	0.9925	12.82	0.03	VLE(DP)
0.8052	11.61	0.05	VLE(BP)				
$T = 358.09 \pm 0.21$							
0.4246	5.14	0.10	VLE(BP)	0.9008	15.21	0.01	VLE(BP)
0.5484	7.06	0.02	VLE(BP)	0.9483	16.02	0.04	VLE(BP)
0.7024	10.75	0.02	VLE(BP)	0.9925	13.74	0.01	VLE(DP)
0.8052	13.20	0.10	VLE(BP)				

3 Standard uncertainties u are $u(T) = 0.5$ K, $u(p) = 0.20$ MPa, $u(x) = 0.005$. σ/MPa represents the standard
4 deviation of triplicate measurements. VLE(BP) represents bubble point transitions and VLE(DP) dew point
5 transitions.

6

7

1 **Table 5**

2 Phase equilibrium measurements for the ternary system $\{CO_2(1) + DES(2) + ethanol(3)\}$ at

3 two different DES to ethanol molar ratios.

x_1	$\overline{x}_2$	p/MPa	σ/MPa	Transition type	x_1	$\overline{x}_2$	p/MPa	σ/MPa	Transition type
				DES to ethanol molar ratio of 1:1 ($z_2 = 0.4960$ and $z_3 = 0.5040$).					
$T = 303.28 \pm 0.24$ K									
0.4475	0.5525	3.48	0.06	VLE(BP)	0.7594	0.2406	5.16	0.06	VLE(BP)
0.5547	0.4453	4.02	0.02	VLE(BP)	0.8501	0.1499	6.02	0.03	VLE(BP)
0.6529	0.3471	4.47	0.05	VLE(BP)	0.9509	0.0491	6.52	0.01	VLE(BP)
$T = 313.17 \pm 0.29$ K									
0.4475	0.5525	4.10	0.10	VLE(BP)	0.7594	0.2406	6.40	0.05	VLE(BP)
0.5547	0.4453	4.81	0.10	VLE(BP)	0.8501	0.1499	7.18	0.02	VLE(BP)
0.6529	0.3471	5.50	0.01	VLE(BP)	0.9509	0.0491	7.87	0.10	VLE(BP)
$T = 323.21 \pm 0.24$ K									
0.4475	0.5525	4.70	0.10	VLE(BP)	0.7594	0.2406	7.43	0.00	VLE(BP)
0.5547	0.4453	5.60	0.10	VLE(BP)	0.8501	0.1499	8.52	0.03	VLE(BP)
0.6529	0.3471	6.22	0.00	VLE(BP)	0.9509	0.0491	9.40	0.09	VLE(BP)
$T = 333.17 \pm 0.26$ K									
0.4475	0.5525	5.29	0.01	VLE(BP)	0.7594	0.2406	8.88	0.05	VLE(BP)
0.5547	0.4453	6.83	0.02	VLE(BP)	0.8501	0.1499	10.09	0.05	VLE(BP)
0.6529	0.3471	7.27	0.05	VLE(BP)	0.9509	0.0491	11.45	0.05	VLE(BP)
$T = 343.16 \pm 0.27$ K									
0.4475	0.5525	5.93	0.03	VLE(BP)	0.7594	0.2406	10.28	0.01	VLE(BP)
0.5547	0.4453	7.63	0.01	VLE(BP)	0.8501	0.1499	11.66	0.06	VLE(BP)
0.6529	0.3471	8.52	0.06	VLE(BP)	0.9509	0.0491	12.84	0.04	VLE(BP)
				DES to ethanol molar ratio of 1:2 ($z_2 = 0.3240$ and $z_3 = 0.6760$).					
$T = 303.28 \pm 0.23$ K									
0.4506	0.5494	3.86	0.02	VLE(BP)	0.7506	0.2494	5.59	0.01	VLE(BP)
0.5505	0.4495	4.44	0.01	VLE(BP)	0.9011	0.0989	5.96	0.04	VLE(BP)
$T = 313.15 \pm 0.17$ K									
0.4506	0.5494	4.46	0.01	VLE(BP)	0.7506	0.2494	6.69	0.02	VLE(BP)
0.5505	0.4495	5.32	0.01	VLE(BP)	0.9011	0.0989	7.37	0.03	VLE(BP)
$T = 323.13 \pm 0.21$ K									
0.4506	0.5494	5.25	0.01	VLE(BP)	0.7506	0.2494	7.89	0.03	VLE(BP)
0.5505	0.4495	6.23	0.06	VLE(BP)	0.9011	0.0989	8.95	0.05	VLE(BP)
$T = 333.15 \pm 0.20$ K									
0.4506	0.5494	6.02	0.02	VLE(BP)	0.7506	0.2494	9.33	0.04	VLE(BP)
0.5505	0.4495	7.33	0.02	VLE(BP)	0.9011	0.0989	10.57	0.02	VLE(BP)
$T = 343.14 \pm 0.35$ K									
0.4506	0.5494	6.85	0.01	VLE(BP)	0.7506	0.2494	10.82	0.04	VLE(BP)
0.5505	0.4495	8.01	0.01	VLE(BP)	0.9011	0.0989	12.24	0.04	VLE(BP)

1   Standard uncertainties u are $u(T)$ = 0.5 K, $u(p)$ = 0.20 MPa, $u(x)$ = 0.005. σ/MPa represents the standard
2   deviation of triplicate measurements. VLE(BP) represents bubble point transitions and VLE(DP) dew point
3   transitions.

1 **Table 6**

2 Phase equilibrium measurements for the ternary system $\{CO_2(1) + DES(2) + ethyl$

3 acetate(3)$\}$ at DES to ethyl acetate molar ratio of 1:1 ($z_2 = 0.4970$ and $z_3 = 0.5030$).

x_1	$\bar{x}_2$	p/MPa	σ/MPa	Transition type	x_1	$\bar{x}_2$	p/MPa	σ/MPa	Transition type
$T = 303.25 \pm 0.10$ K									
0.4655	0.5345	2.75	0.02	VLE(BP)	0.9006	0.0994	5.99	0.02	VLE(BP)
0.8047	0.1953	5.15	0.10	VLE(BP)	0.9466	0.0534	6.45	0.02	VLE(BP)
$T = 313.21 \pm 0.20$ K									
0.4655	0.5345	3.23	0.02	VLE(BP)	0.9006	0.0994	7.07	0.01	VLE(BP)
0.8047	0.1953	6.05	0.03	VLE(BP)	0.9466	0.0534	7.79	0.01	VLE(BP)
$T = 323.06 \pm 0.15$ K									
0.4655	0.5345	3.88	0.01	VLE(BP)	0.9006	0.0994	8.48	0.00	VLE(BP)
0.8047	0.1953	7.06	0.00	VLE(BP)	0.9466	0.0534	9.29	0.05	VLE(BP)
$T = 333.15 \pm 0.18$ K									
0.4655	0.5345	4.39	0.01	VLE(BP)	0.9006	0.0994	10.04	0.04	VLE(BP)
0.8047	0.1953	8.33	0.02	VLE(BP)	0.9466	0.0534	10.77	0.07	VLE(BP)
$T = 343.11 \pm 0.31$ K									
0.4655	0.5345	4.99	0.10	VLE(BP)	0.9006	0.0994	11.70	0.02	VLE(BP)
0.8047	0.1953	9.75	0.06	VLE(BP)	0.9466	0.0534	12.23	0.04	VLE(BP)

4 Standard uncertainties u are $u(T) = 0.5$ K, $u(p) = 0.20$ MPa, $u(x) = 0.005$. σ/MPa represents the standard
5 deviation of triplicate measurements. VLE(BP) represents bubble point transitions and VLE(DP) dew point
6 transitions.

7

8

1

Table 7

Binary interaction parameters for PR-EoS thermodynamic model.

System	T / K	k_{12}	l_{12}	$rmsd$/MPa
$\{CO_2(1)+ \text{ethanol}(2)\}^a$	303 – 343 K	0.0783	-0.0310	0.26
$\{CO_2(1) + \text{ethyl acetate}(2)\}^b$	313 – 353 K	0	0	0.16
		-0.0171	-0.0334	0.10
$\{CO_2(1) + \text{DES}(2)\}^b$	313 – 353 K	0	0	0.49
		-0.0178	-0.0181	0.30

[a] Binary interaction parameters taken from Araújo et al. [29]; [b] This work.

Table 8

Evaluation of binary interaction parameters (k_{23} and l_{23}) for solute – solute interactions.

Pair	T / K	k_{23}	l_{23}	$rmsd$/MPa [a]
DES(2) - ethanol(3)	303 – 343 K	0	0	0.39
		0.1185	0.1126	0.24
DES(2) - ethyl acetate(3)	313 – 353 K	0	0	0.38
		0.1661	0.1149	0.17

[a] $rmsd$ calculated using the entire set of experimental data in Table 5 and Table 6. Binary interaction parameter of CO_2 + ethanol, CO_2 + ethyl acetate and CO_2 + DES were fixed to the fitted values in Table 7.

1
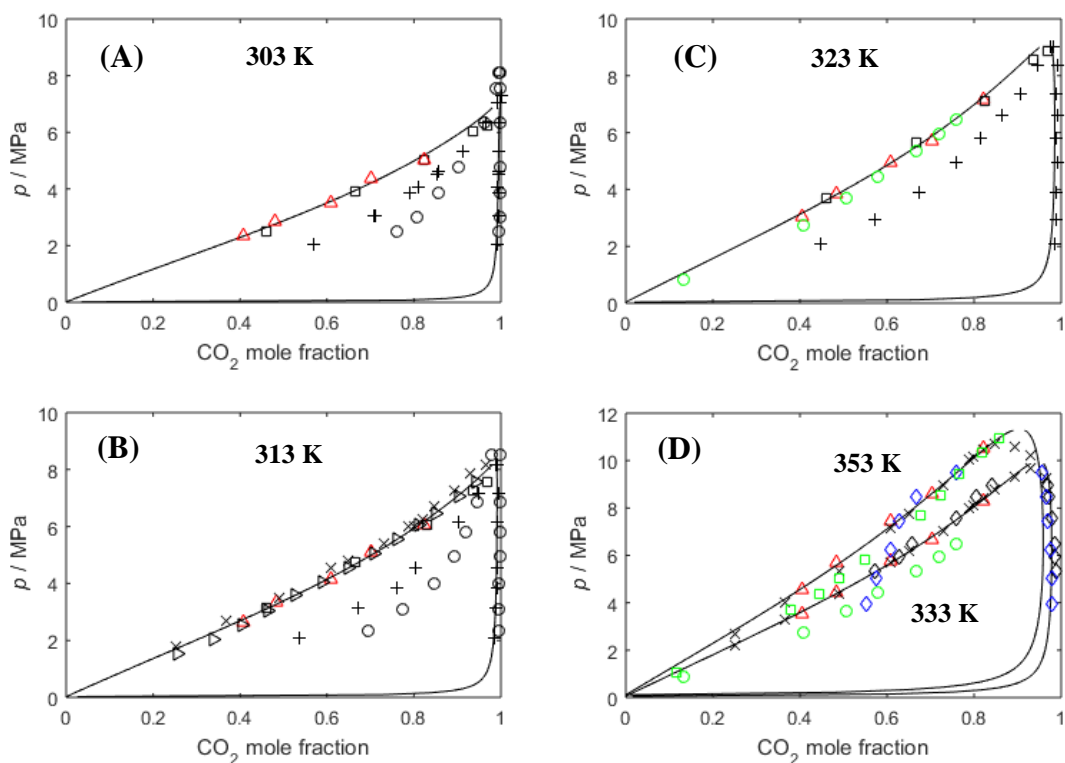
Figure 1

Pressure-composition diagram for the binary system {CO_2(1) + ethyl acetate(2)} at different temperatures. **(A)** 303 K (△, this work; □, Borges et al. [28]; +, Wagner et al. [24]; ○, Silva et al. [25]), **(B)** 313 K (△, this work; □, Borges et al. [28]; ▷, Aida et al. [23]; ×, Byun et al. [22]; +, Wagner et al. [24]; ○, Silva et al. [25]), **(C)** 323 K (△, this work; □, Borges et al. [28]; +, Wagner et al. [24]; ○, Sima et al. [26]) and **(D)** 333 K (△, this work; ×, Byun et al. [22]; ◇, Tian et al. [27]; ○, Sima et al. [26]) and 353 K (△, this work; ×, Byun et al. [22]; ◇, Tian et al. [27]; □, Sima et al. [26]). Continuous lines denote the phase envelop calculated using the PR model ($k_{12} = l_{12} = 0$).

11

12

13

1
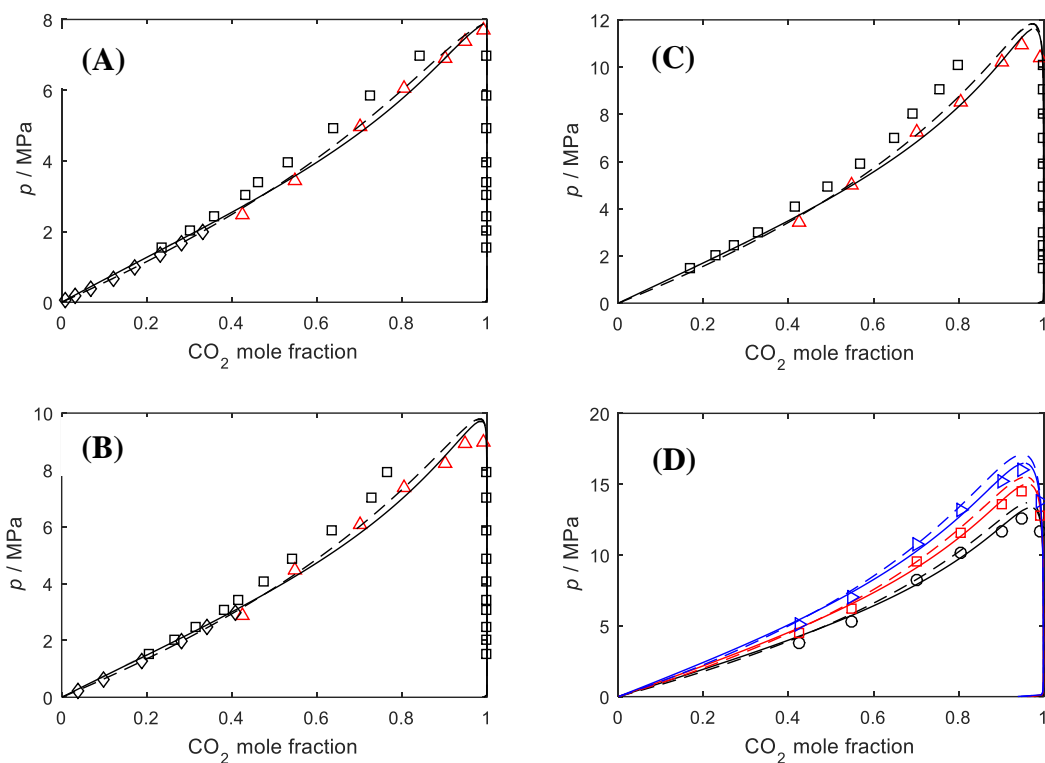
Figure 2

Pressure-composition diagram for the binary system {$CO_2(1)$ + DES(2)} at different temperatures. **(A)** 308 K (△, this work; ▢, Feng et al. [3]; ◇, Li et al. [10], **(B)** 318 K (△, this work; ▢, Feng et al. [3]; ◇, Li et al. [10], **(C)** 328 K (△, this work; ▢, Feng et al. [3]; ◇, Li et al. [10] and **(D)** 338 K (○, this work), 348 K (▢, this work) and 358 K (▷, this work). Continuous lines denote the phase envelop calculated using the PR model with fitted parameters (Table 7) and dashed lines with interaction parameters set to zero ($k_{12} = l_{12} = 0$).

1
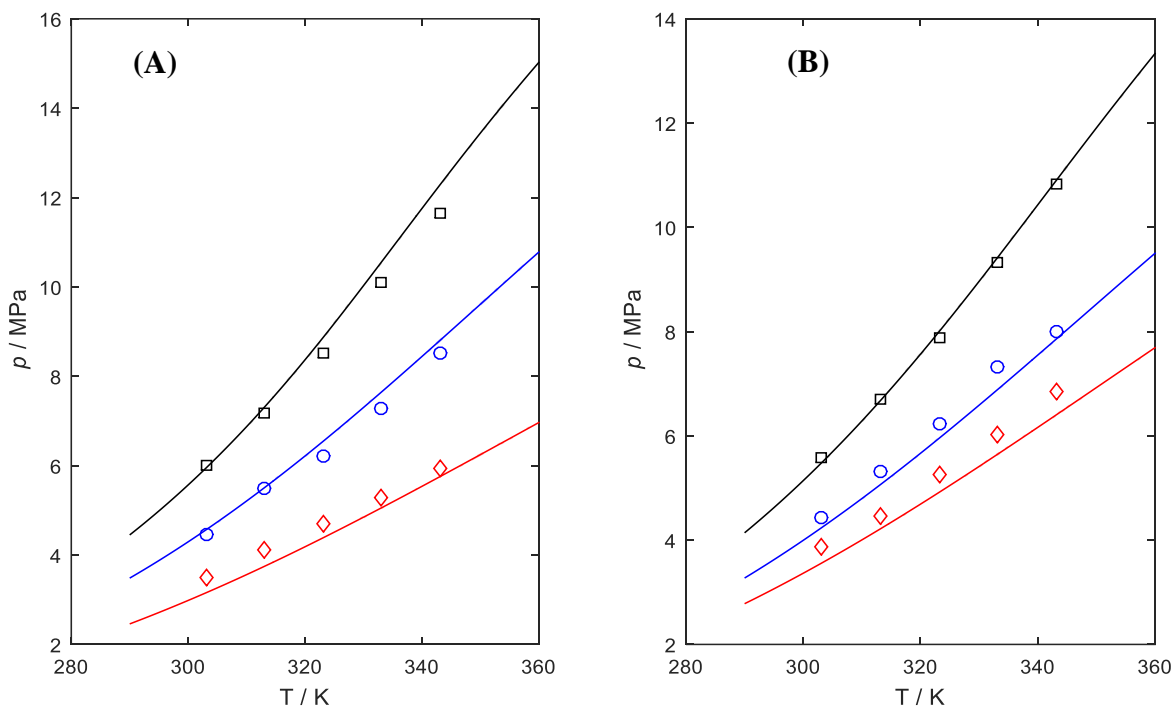
Figure 3

Pressure-temperature diagrams for the ternary system $\{CO_2(1) + DES(2) + ethanol(3)\}$ at different fixed compositions. **(A)** DES to ethanol molar ratio of 1:1 ($\Diamond$, $x_1 = 0.4475$, $x_2 = 0.2740$ and $x_3 = 0.2785$; $\circ$, $x_1 = 0.6529$, $x_2 = 0.1722$ and $x_3 = 0.1749$; $\square$, $x_1 = 0.8501$, $x_2 = 0.0744$ and $x_3 = 0.0755$), and **(B)** DES to ethanol molar ratio of 1:2 ($\Diamond$, $x_1 = 0.4506$, $x_2 = 0.01780$ and $x_3 = 0.3714$; $\circ$, $x_1 = 0.5505$, $x_2 = 0.1456$ and $x_3 = 0.3039$; $\square$, $x_1 = 0.7506$, $x_2 = 0.0808$ and $x_3 = 0.1686$). Experimental measurements (symbols) and comparison with simulated values using the PR model (k_{12}, l_{12}, k_{13} and l_{13} from Table 7 and $k_{23} = l_{23}= 0$).

10

1
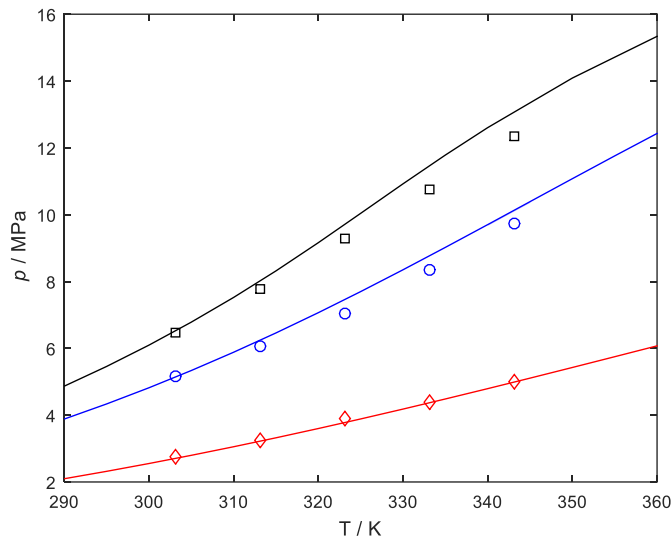
Figure 4

Pressure-temperature diagram for the ternary system $\{CO_2(1) + DES(2) + \text{ethyl acetate}(3)\}$ at different fixed compositions (DES to ethyl acetate molar ratio of 1:1). **(A)** ($\diamond$, $x_1 = 0.4655$, $x_2 = 0.2565$ and $x_3 = 0.2689$; $\circ$, $x_1 = 0.8047$, $x_2 = 0.0969$ and $x_3 = 0.0984$; $\square$, $x_1 = 0.9466$, $x_2 = 0.0265$ and $x_3 = 0.0269$. Experimental measurements (symbols) and comparison with simulated values (solid lines) using the PR model (k_{12}, l_{12}, k_{13} and l_{13} from Table 7 and $k_{23} = l_{23} = 0$).
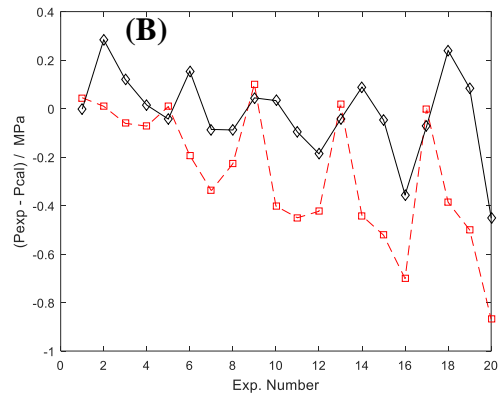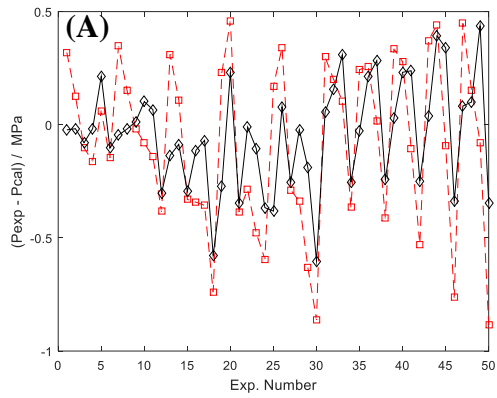
9

10

11

12

30

1

Figure 5

Error ($P_{exp} – P_{cal}$) distribution for the saturation pressure predictions for the ternary systems

(A) {CO_2(1) + DES(2) + ethanol(3)} and **(B)** {CO_2(1) + DES(2) + ethyl acetate(3)}. Red

squares with dashed line represent the error of calculations using interaction parameter k_{23}

= l_{23} = 0, and black diamonds with solid line represent the error of calculations using fitted

values of k_{23} and l_{23} (as presented in Table 8).

8

9